ISSN 1392–1320 MATERIALS SCIENCE (MEDŽIAGOTYRA). Vol. 15, No. 2. 2009

Viscoelastic Behavior of a Single-Crystal Nickel-Base Superalloy

Lembit KOMMEL*

Department of Materials Engineering, Tallinn University of Technology, Ehitajate tee 5, 19086 Tallinn, Estonia

Received 26 November 2008; accepted 03 February 2009

Tensile specimens of an experimental single-crystal nickel-based superalloy with [001] orientation were subjected to cyclic tension-compression loading under strain control regime on materials testing system Instron-8516 at room temperature and ambient atmosphere. Recent research on the viscoelastic behavior of material has shown that their elastic deformation occurs in the initial portion of a stress-strain relationship, which is initially linear up to proportional limit with strain of ~0.55 %. Until then the material show's fully elastic behavior at strain amplitudes of 0 % – 0.05 %, 0 % – 0.2 %, and 0 % – 0.5 % for 30 cycles and corresponding diagrams covers each-other. At the increased strain amplitude of 1 % the elastic limit occurs at first cycle and tensile strain of ~0.65 %. The specimen was plastically deformed from 0.65 % up to 1 % of tension with no load significantly increased. Next 29 cycles were conducted at strain amplitude of 1 %. The strain-stress curves on diagram covers each-other at 1 % of strain value. Material ordinarily possesses upscale elastic behavior stability due largely to improved resistance to deformation of a cuboidal intermetallic γ′-phase. However, under the cyclic straining the dendrite arms were decreased in dimensions about three times as compared to primary dendrite arm. The γ-phase tended to dissolve into the primary cuboidal intermetallic γ′-phase. The cast formed of niobium-tantalum intermetallic inclusions began to dissolve and supplies the γ-matrix during cycling. As a result, the raft microstructure was not formed, as it was usually formed during creep testing at high temperatures.

Keywords: nickel-base single crystal superalloy, hard cyclic viscoplastic deformation, ratchetting, viscoelastic behavior, viscosity.

INTRODUCTION

It is well known, that the cast single crystal (SC) Ni-based superalloys, as functional material with a high stability of strength properties at elevated temperatures [1, 2], have been used up to now to produce turbine blades and vanes of turbo-jets [3] for aircraft and gas turbines [4] for power plants. When exploited, these materials are subjected to complex thermal and mechanical loadings. In a practical application, the turbine blades will experience a complex loading, not only of the uniaxial, but also of the multiaxial nature. A loading frequency of the high cycle torsion and vibration depends on the speed of rotor rotating and the number of blades on turbine disc and in vanes. At the some times the rotor disc blades are heavily loaded under centrifugal power also. These load values depend on radius, weight and rotor rotating speed or turbojet's working regime. Whereas the blades and vanes of turbine worked at condition of a very high gas temperature and relatively low air cooling temperature, for that reason they are heavily loaded under high gradient of thermal ratchetting. Therefore, testing at a one time when all these effects are occurring is considerably complicated. Usually this refractory material can be tested on creep resistance at high temperatures [5 – 15]. The creep depends on temperature, time and the direction of the load applied to single crystal orientation of nickel-based of superalloy cast.

Usually the direction of tension loading accompanied with [001] orientation of SC. Creep resistance is the largest in this direction of SC. During a high temperature creep as result of diffusion aided by tension, the γ'-phase surrounds the γ-phase, and as result, the raft microstructure [4, 12] can be formed. The kinetics of the topological inversion of the γ/γ'-microstructure during creep of a Ni-based superalloy are studied in a large numerous works [4 – 10]. The dislocations climbing and stacking faults of superalloys under high cycle fatigue (HCF) [7], low cycle fatigue (LCF) [8], bending [9], and deformation [10] loadings are studied mainly at elevated temperatures. These testing's are mainly conducted on smooth and notched specimens up to fracture. As knows [13] the SC superalloys might have casting porosity which is predominantly in the interdendritic regions. In the case of high temperature-stress creep conditions vicinity of topologically close packed pores are areas as stress concentration and subjects of creep damage and rafts microstructure forming, also [16]. Unfortunately, at present, these SC Ni-based superalloys are scantily studied at cyclic plasticity condition [17], as well under uniaxial ratcheting [18] and hard cyclic viscoplastic (HCV) deformation [19] also.

The aim of this study is to present the experimental test results of the stress-strain characteristics and elastic behavior, as well as phases and microstructure evolution analyses in experimental SC Ni-based superalloy under cyclic straining of HCV deformation as test method.

EXPERIMENTAL

The experimental SC Ni-base superalloy castings with a diameter of 15 mm and length of 180 mm have been produced by means of electro-induction melting method in a directional solidification furnace under a high vacuum, and solidified in the [001] direction. For present study the cast bars of SC were previously heat treated in vacuum furnace at temperature of ~1000 °C for 5 h. These bars

*Corresponding author. Tel.: +372-6203356, fax.: +372-6203196.
E-mail address: *Lembit.Kommel@ttu.ee* (L. Kommel)

were used for cutting off by turning the tensile test specimens. The tensile specimens with the grip sections have an overall length of 87 mm. The gage part has a length of 12 mm with diameter of 8 mm and a fillet radius of 6 mm.

The SC Ni-based superalloy testing was performed under the controlled regime of strain amplitude on materials testing system Instron-8516. For a true strain measure, the extensometer with the base length of 10 mm was used. The testing was conducted by the HCV deformation [19] test method at a room temperature. Cyclic loading was applied at the tension-compression with steps of strain amplitudes of 0 %– 0.05 %; 0 %– 0.2 %; 0 %– 0.5 % and 0 %– 1 % for 30 cycles at each strain value. The tension loading was conducted under low frequency of 0.5 Hz and, consequently at increased strain velocity for each step. For each cycle the 100 test points of displacement and load for time were measured automatically.

For the microstructure evolutions during straining study, the cuts, which were cat off from different part of samples before and after straining were mechanically polished and etched. For dissolving out of γ'-precipitates the chemical compound (33 ml HNO_3 and 66 ml HCl) was applied. The dendrite macroarchitecture of samples was analyzed by using the light optical microscope Nikon Microphot-FX. The microstructure of samples was analyzed by the high resolution field emission scanning electron microscopy (FE SEM) Zeiss ULTRA-55 equipped with the In-Lens secondary electrons (SE) detector for topographic imaging and energy, and the angle selective backscattered electrons (EsB) for the compositional contrast. The profundity of dissolving of single γ'-phase area, metal carbides (MC) and γ'-precipitates in a γ-channels was analyzed by the atomic force microscope (AFM) NT-MDT Smena SFC050L. The tip of AFM has the radius of 10 nm, the height about 20 μm and corner about 22 degrees.

RESULTS AND DISCUSSION

The summary graphic of strain-stress curves of cyclic straining of the SC superalloy is shown in Fig. 1. At the minimal tensile strain amplitude of 0 %– 0.05 % the received strain-stress curve exhibits the linear dependence. The maximal stress was 75 MPa at tension. By an increased strain of 0.2 % the stress was increased up to 300 MPa, and for the strain of 0.5 % up to 760 MPa in mean. In the diagram, the strain-stress curves at these strain values cover each other. At the strain amplitudes of 0 %– 0.05 % (curve 0-I), 0 %– 0.2 % (curve 0-II) and 0 %– 0.5 % (curve 0-III) the material shows a fully elastic behavior for 30 cycles, respectively. During the first cycle, for each of these test series of straining, as a system error, the strain (and load equally) was higher up to 5 % as the maximum in comparison with the values of following cycles. This value for fourth series is shown (in Fig. 1) as ΔS. At this stage of the straining, the curves are approximately identical to a ratchetting behavior, but only without elongation of gauge length of sample. By the strain amplitude increasing up to 1 % during the first cycle at the next stage, the flow curve shows a light sliding behavior ranging from 0.65 % to 1.03 % at tensile straining (see Fig. 1). Plastic deformation of SC was started at the elastic

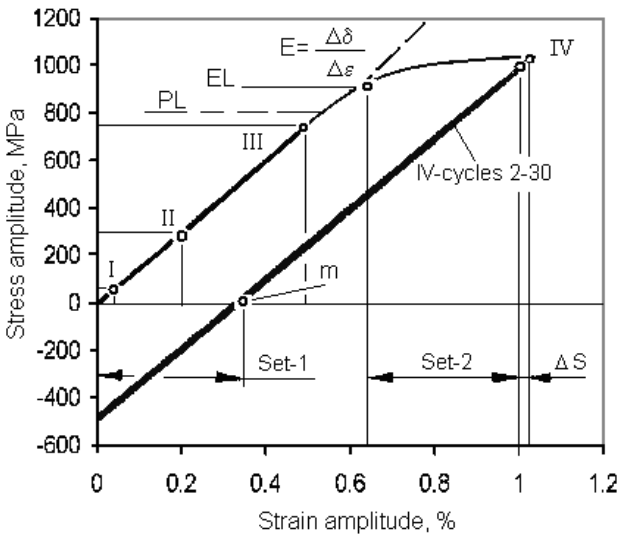

Fig. 1. This graph gives a summary of the strain-stress behavior of the SC Ni-based superalloy under hard cyclic loading. The definitions are as follows: PL – proportional limit; EL – elastic limit, 0-I – strain-stress curve at the strain amplitude of 0 %– 0.05 % for 30 cycles; 0-II – at 0 %– 0.2 %; 0 – III – at 0 %– 0.5 %; 0 – IV – tension curve of first cycle at strain of 1 %; and IV – cycles 2 – 30 – strain stress curves at strain amplitude of 1 %; ΔS ~0.03 % of strain (as system error); Set-1 ≈ Set-2 – plastic deformation part at first cycle of the fourth test series

limit (EL) with the tensile strain of 0.65 % during first cycle of straining at fourth series (Fig. 1, curve EL-IV). At very first cycle of straining the elastic deformation of SC Ni-based superalloy with stress amplitude from 1022 MPa at tension to 484 MPa at compression was conducted. During next 29 cycles of straining the elastic deformation of SC the stress at tension was decreased to 1000 MPa and the stress at at compression increased to 492 MPa in mean (Fig. 1, bold line, IV –cycles 2 – 30). As the sample was plastically deformed in length (Set-2 ≈ 0.35 %) the stress-strain curve (IV – cycles 2 – 30) in the point "m" segments the *x*-axis on Set-1 section. After this the material shows the asymmetric but fully elastic behavior under tension-compression loading or so called HCV deformation [19]. During hard cyclic loading under the strain amplitude of ±1 % the tensile stress is approximately two times higher than the compressive stress (see Fig. 1, σ_T = 1022 MPa and σ_C = 492 MPa). During such straining the dimensions of test samples were no changed and fracture no occurred.

After preliminarily heat treatment at temperature of 1000 °C for 5 h in vacuum furnace the macroarchitecture studied by the optical light microscope in direction [001] of tensile specimen (before straining) from cast SC Ni-based superalloy contains primary dendrites with arm of different configurations (Fig. 2, a). During cycling, the dendrites were decreased in dimensions down to 2–3 times (Fig. 2, b) compared to the no cyclically loaded SC material. These optical microscope pictures (Fig. 2) are conducted from one tensile specimen after HCV deformation. By this the picture (see Fig. 2, a) was conducted from grip section and picture (see Fig. 2, b) from gage section of specimen. Such microstructure evolution was conducted on all length of gage but not at middle part of this only. The dimensions of dendrite arms in the cyclically loaded

condition are lowered as result of diffusion aided by cyclic deformation. The research shows that the γ'-precipitates are sheared by the anti-phase boundaries within γ-phase. The deformed microstructure after low-cycle fatigue (LCF) in a fourth-generation Ni-base SC superalloy TMS-138 was studied in [8] and show, that a large number of stacking faults (SFs) in the matrix at 1073 K and the more competed rafts and smaller interfacial dislocation spacing at 1373 K were formed. By this in [2] is shown, that under high cycle fatigue behavior of a SC superalloy at elevated temperatures in ambient atmosphere the primary cuboidal γ'-precipitates tended to dissolve into the matrix channels or in γ-phase. The large number of secondary γ'-particles were formed into the γ-matrix. In [2, 8] is shown also, that such changes in microstructure have a significant and different impact on the mechanical properties of the SC material.

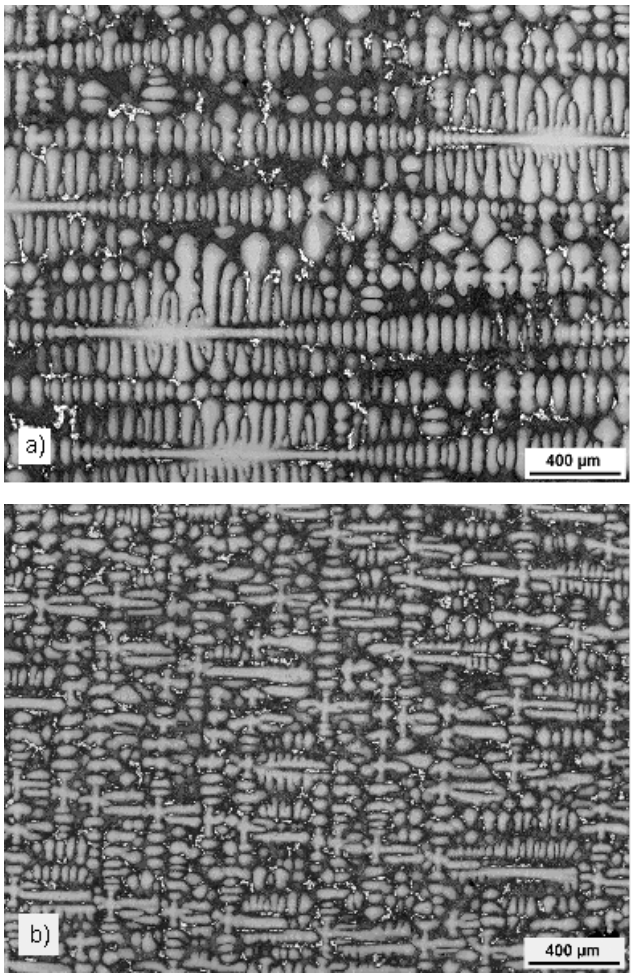

Fig. 2. Optical pictures of microstructure of SC Ni-based superalloy before (a) and after (b) HCV deformation. The crystal growth [001] direction is oriented in horizontals

The microarchitecture in optical picture (Fig. 3) of SC specimen with the different dendritic structure elements contains different chemical compounds also. Dendrite arms contain fine cuboidal γ+γ'-phase microstructure (I). Between the dendrites there is an area with a dispersed γ-phase in γ′-phase (II), γ′-single-phase area with γ precipitates (III) and metal carbides (IV). By applying the FE SEM study of microstructure, there were detected the intermetallic Ta-Nb compounds (Fig. 4 and Table 1, N5) in γ matrix.

Detailed observations of the microstructure of the specimens before and after HCV deformation were performed by FE SEM and AFM use. Was verified by FE SEM study that the microstructure of SC Ni-based superalloy consisted of cuboidal γ'-precipitates with an average size of about 400 nm – 600 nm and separated by γ-channels with a thickness of about 40 nm. These dimensions were very different and depended on the study point on dendrite (see Fig. 3, I). The calculation shows that the volume fraction of the γ'-phase is about 60 %.

The main compositions of chemical elements of phases are listed in Table 1. As is listed in Table 1, the experimental SC Ni-based superalloy does not contain titanium (Ti) as alloying element for other referred [1 – 17] SC superalloys.

For the phase analysis in future, the diamond polished surface of specimens was chemically etched, and as result, the γ'-phase was deepened significantly, corresponding to the γ-phase (Fig. 5, a, b, and Fig. 6).

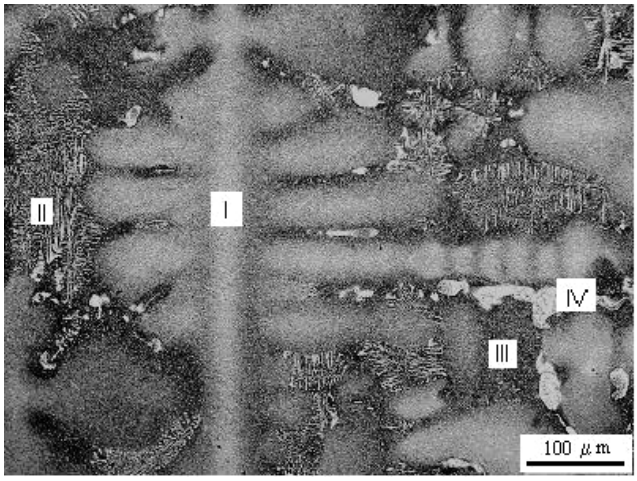

Fig. 3. The morphology of SC superalloy with main phases indicating in interdendritic region is presented in optical picture. Designations: I – dendrite arm with fine cuboidal γ+γ' phase microstructure; II – γ precipitates in single γ' phase (see Fig. 5, b); III – γ- in γ'-eutectics and IV – MC carbide

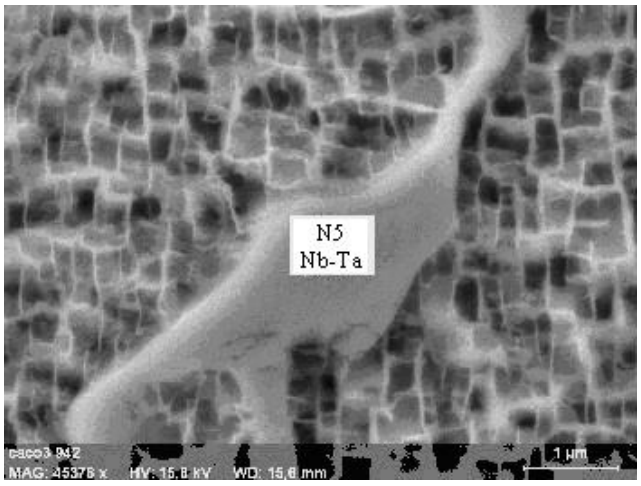

Fig. 4. FE SEM picture of Nb-Ta intermetallic compound (see Table 1, position N5) in γ/γ'-phase matrix

Table 1. Summarized results of chemical composition of phases in atomic (at. %) and weight (wt. %) percentages.

At. %	Ni	Al	W	Cr	Co	Mo	Re	Nb	Ta
N1	64	13	3	6.5	10.7	1	1.7	–	–
N2	62.8	16	4.3	6.9	8.9	1.1	–	–	–
N3	66.9	19	0.4	3	7	–	–	2.1	2
N4	32.9	6.7	6.2	9.3	7.6	–	–	26.9	10.4
N5	–	–	–	–	–	–	–	57	43
Wt. %	**Ni**	**Al**	**W**	**Cr**	**Co**	**Mo**	**Re**	**Nb**	**Ta**
N1	62.3	5.9	9.1	5.6	10.5	1.5	5.1	–	–
N2	62.5	7.3	13.5	6	8.9	1.8	–	–	–
N3	69.7	8.9	1.3	2.8	7.2	–	–	3.7	6.4
N4	22.7	2.1	13.1	5.7	5.3	–	–	19.1	21.5
N5	–	–	–	–	–	–	–	40.5	59.5

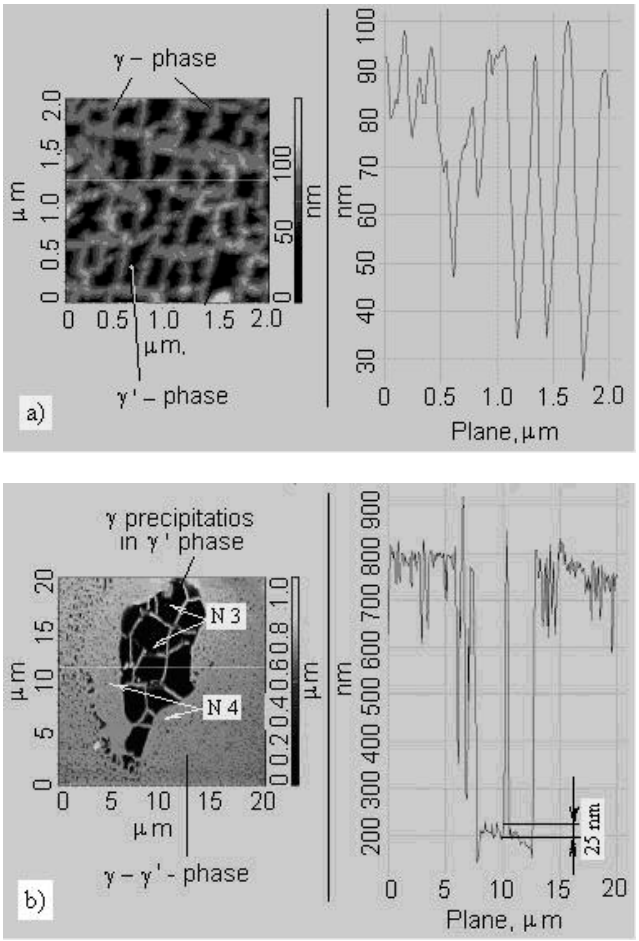

Fig. 5. AFM investigation of SC etching for conduction of phase analyze in γ/γ'-phase (a) and γ precipitations in γ' phase eutectics (b) regions

Whereas the titanium have a low interatomic interaction power and the introduction of titanium as an alloying element of superalloy can be decrease the creep resistance at high temperatures and, consequently, increases the intensive forming of the raft microstructure in material. By this at present study the experimental material contains niobium (Nb) and tantalum (Ta) simultaneously. These metals are not jointly listed in referred [1 – 10, 13, 15] articles but these elements are always jointly in nature and can be formed high stabile intermetallic compounds. In the study [1] is shown, that for single crystal turbine blades best alloying elements are W, Ta and Re. These chemical elements are used for alloying of experimental SC superalloy (see Table 1). During hard cycling loading the phases chemical composition was not changed significantly. The Ni content was increased for single γ′-phase area in mean of 2 % while other elements were decreased within limits of 0.3 %.

The single γ′-phase area (Fig. 5, b) was surrounded by Nb-Ta-rich content. Chemical elements composition is presented in Table 1, position N4.

In dendrite region for γ/γ'-area the Ni and Re contents were decreased within limits of 0.3 % by lightly increasing of Al, W, Cr and Mo contents.

The Nb-Ta inclusions were conducted in the dendrite γ/γ'-areas (see Fig. 4, Table 1, position N5) as well as before and after HCV deformation. They have linear dimension from 1 μm to 5 μm in mean, but were decreased in dimensions during cycling. By this, during cycling the Ta content was increased with compare to Nb content be within limits of 1 wt.%.

The AFM study shows, that the morphology of the interdendritic region of the cast SC superalloy is preferably irregular. The surface roughness as well as the increasing differences between the phases height were quite large. Mainly the γ'-phase (Fig. 5, a) was etched out in a depth of 70 nm, and single γ'-phase eutectic region was etched out in depth of 600 nm (Fig. 5, b). Obviously the depth of γ'-phase in γ/γ'- and single γ'-phase may be higher. The sidewalls of the matrix channels influence the punctual deep measure of γ'-phase. This means that the depth is underestimated, as the tip of cantilever have corner of 22 degrees. The microstructure investigation of SC under different directions shows that they have cuboidal in view channels and consequently the maximum depths of channels correspond approximately to the width of cuboidal γ′-precipitations.

As it is shown in FE SEM picture (Fig. 6), the cuboidal precipitations of γ'-phase were fully etched out from the γ-phase matrix channels (see Fig. 5, a). As it is

shown in Fig. 5, b, the channels walls have network of stacking faults with height of 25 nm – 50 nm. During HCV deformation under shear stresses in direction of [001] (horizontal in Fig. 2), the cross-shaped lines of sliding and dislocation network can be formed [2], but were not conducted by FE SEM study. As it is shown in Fig. 7 the matrix of γ-phase was significantly changed at diffusion during HCV deformation. As was conducted the γ-matrix was dissolved off into cuboidal γ'-phase, and as a result, the γ/γ'-phase microstructure has turbid appearance after HCV deformation. The raft microstructure was not formed, as well as during a high temperature creep testing [1 – 9, 13 – 15] when the material softening process takes place. Contrariwise, during HCV deformation hardening-softening of SC Ni-based superalloy did not appear.

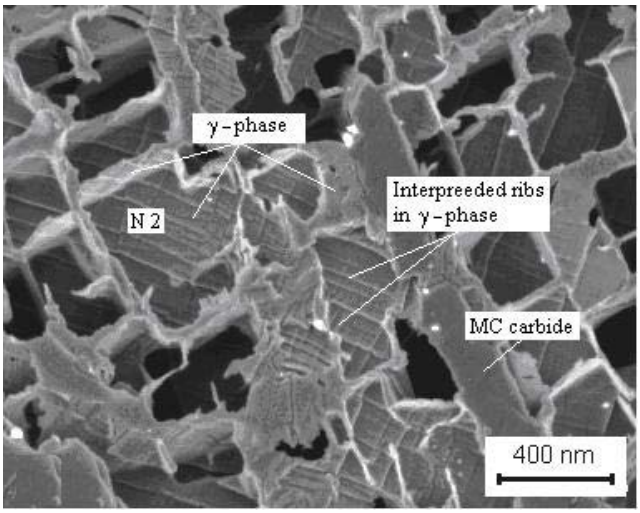

Fig. 6. The γ-phase (see Table 1, N2) in as-cast and heat treated SC superalloy in FE SEM picture is shown. The cuboidal precipitations of γ′-phase were etched off

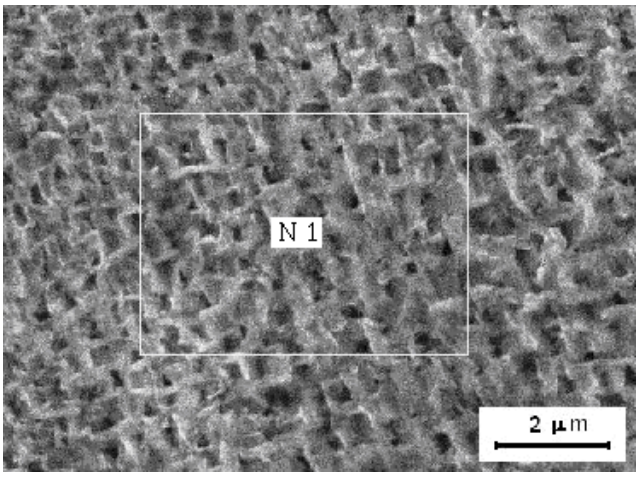

Fig. 7. HCV deformed and diffusive γ/γ'-phase (see Table 1, N1) microstructure from dendrite arm region of SC superalloy

As a result, the diffusion of Nb-Ta intermetallide compounds (aided by cyclic deformation) can be dissolved in the γ-matrix and supplied it. The flow stress of the γ′-precipitates increases with an increase in strain amplitude. By using the EDS method, the chemical compositions of phases (see Table 1) was tested (see Fig. 1, position I) in γ/γ'-phase (Table 1 and Fig. 7 as position N1), γ-phase after etching (Fig. 6 and Table 1 as position N2), single γ'-phase area (Fig. 5, b and Table 1 as position N3), Nb-Ta rich precipitates in the region near γ' single phase area (Fig. 5, b and Table 1, N4) and Nb-Ta intermetallic precipitates area (Fig. 4 and Table 1, position N5). The chemical elements contained these regions (see Fig. 3) are listed in Table 1. As a result of cyclic straining, the chemical content of phases was slightly changed only.

The main elements as those of Ni, Co, and Re were decreased and Al, W, and Cr increased under cyclic loading in test regions. After cyclic loading, a similar effect of the Ta-Nb concentration on the viability of the γ-matrix was found. The roles of Ta and Nb, as transition metals are dissolve and diffuse in γ-matrix. This process increases under cyclic straining. The metallographic characterization of microarchitecture shows that after such hard straining, the dendrites measures in microarchitecture of SC superalloy were changed and decreased significantly and by these phases of the state were slightly changed only at diffusion, which was aided by HCV deformation.

CONCLUSIONS

The SC Ni-based superalloy during HCV deformation at room temperature shows:

– a fully elastic behavior up to strain of 0.65 % and after elongation at first cycle – up to strain of 1 %;

– that under cycling at viscoplastic condition the deformation hardening-softening of SC Ni-based superalloy did not appear;

– that the raft microstructure was not formed;

– the primary dendrites were decreased in dimensions up to two-three times;

– the γ-matrix was dissolved into cuboidal γ'-phase, and as a result, the γ/γ'-phase microstructure has turbid appearance after hard cyclic viscoplastic deformation;

– that the Nb/Ta-intermetallic compound is a key factor for preventing of microstructure and properties stability.

Acknowledgements

Financial support from the Estonian State Science Foundation under Grant of SF140062s08 is appreciated.

REFERENCES

1. **Razumovskii, I. M., Ruban, A. V., Razumovskiy, V. I., Logunov, A. V., Larionov, V. N., Ospennikova, O. G., Poklad, V. A., Johansson, B.** New Generation of Ni-based Superalloys Designed on the Basis of First-principles Calculations *Materials Science and Engineering A* 497 2008: pp. 18 – 24.
2. **Liu, Y., Yu, J. J., Xu, Y., Sun, X. F., Guan, H. R., Hu, Z. Q.** High Cycle Fatigue Behavior of a Single Crystal Superalloy at Elevated Temperatures *Materials Science and Engineering* A 454 – 455 2007: pp. 357 – 366.
3. **Hashizume, R., Yoshinari, A., Kiyono, T., Murata, Y., Morinaga, M.** Development of Ni-based Single Crystal Superalloys for Power-generation Gas Turbines. In: K. A. Green, T. M. Pollock, H. Harada, T. E. Howson, R. C. Reed,

J. J. Schirra, and S. Walston (eds.) *Superalloys 2004 TMS* 2004: p. 53.

4. **Murakumo, T., Kobayashi, Koizumi, T. Y., Harada, H.** Creep Behavior of Ni-based Single-crystal Superalloy with Various γ' Volume Fraction *Acta Materialia* 52 2004: pp. 3737 – 3744.
5. **Rae, C. M. F., Reed, R. C.** Primary Creep in Single Crystal Superalloys: Origins, Mechanisms and Effects *Acta Materialia* 55 2007: pp. 1067 – 1081.
6. **Lukáš, P., Kunz, L., Svoboda, M.** High Cycle Fatigue of Superalloy Single Crystals at High Mean Stress *Materials Science and Engineering* A 387 – 389 2004: pp. 505 – 510.
7. **Zhaokuang, C., Jinjiang, Y., Xiaofeng, S., Hengrong, G., Zhuangqi, H.** High Cycle Fatigue Behavior of a Directionally Solidified Ni-base Superalloy DZ951 *Materials Science and Engineering* A 496 2008: pp. 355 – 361.
8. **Zhou, H., Ro, Y., Harada, H., Aoki, Y., Arai, M.** Deformation Microstructures After Low-cycle Fatigue in a Fourth-generation Ni-base SC Superalloy TMS-138 *Materials Science and Engineering* A 381 2004: pp. 20 – 27.
9. **Tamaki, H., Fujita, K., Okayama, A., Matsuda, N., Yoshinari, A., Kakehi, K.** A Study on Bending Deformation Behavior of Ni-based DS and SC Superalloys In: K. A. Green, T. M. Pollock, H. Harada, T. E. Howson, R. C. Reed, J. J. Schirra and S. Walston (eds.) *Superalloys 2004 TMS* 2004: p. 137.
10. **Coujou, A., Benyoucef, M., Clément, N.** TEM «in situ» Deformation at Room Temperature of a γ/γ′ Superalloy: Propagation of Dislocations in γ Channels *Solid State Phenomena* 35 – 36 1993: pp. 455 – 460.
11. **Epishin, A., Link, T.** Mechanism of High Temperature Creep of Nickel-base Superalloys Under Low Applied Stress. In: K. A. Green, T. M. Pollock, H. Harada, T. E. Howson, R. C. Reed, J. J. Schirra and S. Walston (eds.) *Superalloys 2004 TMS* 2004: p. 137.
12. **Cormier, J., Milhet, X., Mendez, J.** Anisothermal Creep Behavior at Very High Temperature of a Ni-based Superalloy Single Crystal *Materials Science and Engineering A* 483 – 484 2008: pp. 594 – 597.
13. **Reed, R. C., Cox, D. C., Rae, C. M. F.** Damage Accumulation During Creep Deformation of a Single Crystal Superalloy at 1150 °C *Materials Science and Engineering* A 448 1 – 2 2007: pp. 88 – 96.
14. **Inoure, T., Tanaka, K., Adachi, H., Kishida, K., Inui, H.** Effect of Creep Deformation on the Crystallographic Orientation Distribution in Ni Base Superalloy *Advanced Materials Research* 26 – 28 2007: pp. 213 – 216.
15. **Li, S., Tao, J., Sugui, T., Zhuangqi, H.** Influence of Precipitate Morphology on Tensile Creep of a Single Crystal Nickel-base Superalloy *Materials Science and Engineering* A 454 – 455 2007: pp. 461 – 466.
16. **Cormier, J., Villechaise, P., Milhet, X.** γ′-phase Morphology of Ni-based Single Crystal Superalloys as an Indicator of the Stress Concentration in the Vicinity of Pores *Materials Science and Engineering A* (2008) doi:10.1016/j.msea. 2008.10.017. (Accepted).
17. **Jia, Y., Morrison, D. J., Moosbrugger, J. C.** Cyclic Plasticity of Single Crystal Nickel Oriented for Single Slip *Materials Science and Engineering* A 492 2008: pp. 80 – 87.
18. **Chen, G., Chen, X., Niu, C-D.** Uniaxial Ratcheting Behavior of 63Sn37Pb Solders with Loading Histories and Stress Rates *Materials Science and Engineering* A 421 2006: pp. 238 – 244.
19. **Kommel, L.** The Effect of HCV Deformation on Hardening/Softening of SPD Copper. In: Y. T. Zhu, T. G. Langdon, R. Z. Valiev, S. L. Smetanin, D. H. Shin and T. C. Lowe (eds.) *Ultrafine Grained Materials III* TMS 2004: pp. 571 – 576.

Presented at the 17th International Conference "Materials Engineering'2008"
(*Kaunas, Lithuania, November 06 – 07, 2008*)

DOI: 10.5755/j02.ms.26132